J. Fluid Mech. (1997), *vol.* 343, *pp.* 317–330. Printed in the United Kingdom

Inertial effect on the stability of viscoelastic cone-and-plate flow

By DAVID O. OLAGUNJU†

Department of Mathematics, Virginia Polytechnic Institute and State University, Blacksburg, VA 24061-0123, USA

(Received 20 April 1996 and in revised form 10 March 1997)

The stability of axially symmetric cone-and-plate flow of an Oldroyd-B fluid at non-zero Reynolds number is analysed. We show that stability is controlled by two parameters: $\mathscr{E}_1 \equiv DeWe$ and $\mathscr{E}_2 \equiv Re/We$, where De, We, and Re are the Deborah, Weissenberg and Reynolds numbers respectively. The linear stability problem is solved by a perturbation method for $\mathscr{E}_2$ small and by a Galerkin method when $\mathscr{E}_2 = O(1)$. Our results show that for all values of the retardation parameter β and for all values of $\mathscr{E}_2$ considered the base viscometric flow is stable if $\mathscr{E}_1$ is sufficiently small. As $\mathscr{E}_1$ increases past a critical value the flow becomes unstable as a pair of complex-conjugate eigenvalues crosses the imaginary axis into the right half-plane. The critical value of $\mathscr{E}_1$ decreases as $\mathscr{E}_2$ increases indicating that increasing inertia destabilizes the flow. For the range of values considered the critical wavenumber k_c first decreases and then increases as $\mathscr{E}_2$ increases. The wave speed on the other hand decreases monotonically with $\mathscr{E}_2$. The critical mode at the onset of instability corresponds to a travelling wave propagating inward towards the apex of the cone with infinitely many logarithmically spaced toroidal roll cells.

1. Introduction

The flow of a viscoelastic fluid sheared between a cone and a plate has important applications in rheometry. In steady shear rheometry it is assumed that the flow remains stationary. Experiments, however, show that at high shear rates the stationary viscometric flow is unstable (Magda & Larson 1988; McKinley *et al.* 1991; McKinley *et al.* 1995). The first analysis of the stability of cone-and-plate flow of an Oldroyd-B fluid was done by Phan-Thien (1985). Later, Olagunju & Cook (1993) analysed the problem taking into account the weak secondary flow. Both of these analyses were restricted to a class of von Kármán similarity solutions. Phan-Thien (1985) assumed that the Reynolds number was zero and showed that the base flow loses stability when the Deborah number, De, increases past a critical value given by $De_c = \pi(2/5\beta)^{1/2}$. Olagunju & Cook (1993) obtained for creeping flow (i.e. Reynolds number $Re = 0$) the critical Deborah number $De_c = \pi[2/(\beta(3 + 2\beta)]^{1/2}$. The discrepancy in the two critical Deborah numbers is probably due to the fact that Olagunju & Cook took into account the weak secondary flow. In Olagunju & Cook (1993) and Phan-Thien (1985) it was shown that as the Deborah number increases past the critical value a

† Permanent address: Department of Mathematical Sciences, University of Delaware, Newark, DE 19716, USA.

real eigenvalue crosses the imaginary axis into the right half-plane leading to a loss of stability. A bifurcation analysis of this problem has been done by Olagunju (1995*a*).

Contrary to the results predicted by the analyses referred to above, recent experiments have shown that at a critical Deborah number the base flow loses stability to a time-periodic solution and not to another stationary solution (Magda & Larson 1988; McKinley *et al.* 1991, 1995). In addition, the solutions that bifurcate do not correspond to solutions of von-Kármán similarity type. A numerical analysis of the full linear stability problem for creeping flow was carried out by McKinley *et al.* (1995). Olagunju (1995*b*) obtained analytical results for the stability problem for an Oldroyd-B fluid. Although the analysis assumed that the gap angle is small, his results, based on a short-wave model, agree very well with those obtained numerically in McKinley *al.* (1995). Olagunju (1997) analysed the Hopf bifurcation problem for $Re = 0$. Purely elastic instabilities have been observed and analysed for other flows including parallel plate flow (Byars *et al.* 1994), the Taylor–Couette flow (Larson, Shaqfeh & Muller 1990) and the Taylor–Dean flow (Joo & Shaqfeh 1992). Joo & Shaqfeh (1994) have also analyzed the effect of inertia on the Taylor–Dean flow.

In this paper we examine the linear stability problem for cone-and-plate flow of an Oldroyd-B fluid when the Reynolds number is non-zero. This problem will be solved using a perturbation method when inertia is small and a Galerkin method when the Reynolds number is not necessarily small. Some results for the upper convected Maxwell model were reported in Olagunju (1996). Our results show that inertia tends to destabilize the flow. We also show that the wavenumber of the most unstable mode first decreases and then increases as inertia increases. The speed of travelling waves on the other hand decreases with increasing inertia.

In this paper we will consider only axially symmetric perturbations. Although the experiments reported by McKinley *et al.* (1995) show that for the particular fluid used, the most unstable mode was a non-axially symmetric logarithmic spiral wave, their linear stability analysis does not however preclude bifurcations to axisymmetric travelling waves. What they found was that the most unstable mode was strongly dependent on fluid rheology and cone size. Their linear stability analysis shows that for a fluid with solvent viscosity (in our notation) $\beta < 0.4$, the most unstable modes were axially symmetric. In their experiments they observed axisymmetric waves when the conical fixture was 6° for a fluid with $\beta = 0.16$. For a fluid with $\beta = 0.41$ they observed mostly non-axisymmetric spirals but even in this case they reported that sometimes they saw both axially symmetric and non-axially symmetric modes coexist suggesting possible mode interactions. In McKinley *et al.* (1995), it was reported that S. J. Muller had also observed axisymmetric instabilities in experiments with a cone-and-plate device. In addition Byars *et al.* (1994) observed axisymmetric vortices in experiments with parallel plates. They also noted that in some cases both axisymmetric and non-axisymmetric modes appeared to coexist. The only way to resolve the issue satisfactorily is to do a nonlinear analysis. Inertial effects on non-axisymmetric disturbances are currently under investigation.

2. Problem formulation

Consider a cone-and-plate system with gap angle α in which the cone is rotated at a constant angular speed ϖ. The equations governing the flow of are (Bird, Armstrong & Hassager 1987),

$$\nabla \cdot \tilde{\boldsymbol{v}} = \boldsymbol{0}, \tag{2.1}$$

$$\tilde{\rho}\frac{\mathrm{D}\tilde{\boldsymbol{v}}}{\mathrm{D}t} = -\nabla\tilde{p} + \nabla\cdot\tilde{\boldsymbol{T}}. \tag{2.2}$$

For the constitutive law we use the Oldroyd-B model for which the stress can be written

$$\tilde{\boldsymbol{T}} = 2\eta_s\boldsymbol{D} + \tilde{\boldsymbol{\tau}} \tag{2.3}$$

where $\tilde{\boldsymbol{\tau}}$, the Maxwell stress, satisfies the equation

$$\tilde{\boldsymbol{\tau}} + \lambda\left(\frac{\mathrm{D}\tilde{\boldsymbol{\tau}}}{\mathrm{D}\tilde{t}} - \boldsymbol{L}\tilde{\boldsymbol{\tau}} - \tilde{\boldsymbol{\tau}}\boldsymbol{L}^T\right) = 2\eta_p\boldsymbol{D}. \tag{2.4}$$

Here $\tilde{\boldsymbol{v}}$ is the velocity, $\tilde{p}$ is the pressure, $\tilde{\rho}$ is the density, λ is the relaxation time, η_s is the solvent viscosity and η_p is the polymer viscosity; $\boldsymbol{L}$ is the velocity gradient tensor and $\boldsymbol{D}$ its symmetric part. The above system of equations is to be solved subject to no-slip conditions at the solid boundaries. Let $(\tilde{r}, \phi, \theta)$ be spherical coordinates. The problem is to be solved in the domain

$$0 \leqslant \tilde{r} \leqslant a, \quad (\pi/2 - \alpha) \leqslant \phi \leqslant \pi/2, \quad 0 \leqslant \theta \leqslant 2\pi.$$

The analysis of (2.1)–(2.4) is very intractable. In Olagunju (1995*b*) a perturbation technique based on a short-wave analysis was used to obtain a set of equations which is more tractable. With some modification that analysis can be extended to the case where the Reynolds number $Re \neq 0$.

Following Olagunju (1995*b*) we non-dimensionalize as follows:

$$\tilde{r} = \alpha a r, \quad \dot{\gamma}\tilde{t} = t, \quad \tilde{p} = \eta\dot{\gamma}p, \tag{2.5}$$

$$\tilde{\boldsymbol{v}} = \alpha a\varpi(ru, rv, rw) \tag{2.6}$$

$$\boldsymbol{\tau} = \eta\dot{\gamma}\begin{pmatrix} \Sigma & \zeta & \gamma \\ \zeta & \Gamma & \Pi \\ \gamma & \Pi & \Delta/\alpha \end{pmatrix}, \tag{2.7}$$

where ϖ is the angular speed of the cone, $\dot{\gamma} = \varpi/\alpha$ is the shear rate and a is the plate radius. It has been shown (McKinley *et al.* 1991, 1995, Olagunju 1995*b*) that the most dangerous modes have short wavelengths with wavenumbers of $O(\alpha^{-1})$. Consequently in Olagunju (1995*b*) we adopted the scaling $r = \rho^\alpha$ and for convenience we let $\psi = (\pi/2 - \phi)/\alpha$ so that $\psi = 0$ on the plate and $\psi = 1$ on the cone. Note that ρ is not related to the density $\tilde{\rho}$. The domain of the problem is now

$$0 \leqslant r \leqslant 1/\alpha, \quad 0 \leqslant \psi \leqslant 1, \quad 0 \leqslant \theta \leqslant 2\pi.$$

2.1. *Small gap theory*

Following Olagunju (1995*b*), and assuming axial symmetry, the leading-order equations for $\alpha \ll 1$, are

$$\rho\frac{\partial u}{\partial\rho} - \frac{\partial v}{\partial\psi} = 0, \tag{2.8}$$

$$Re\left(\frac{\partial u}{\partial t} + u\rho\frac{\partial u}{\partial\rho} - v\frac{\partial u}{\partial\psi}\right) = -\rho\frac{\partial p}{\partial\rho} + \rho\frac{\partial\Sigma}{\partial\rho} - \frac{\partial\zeta}{\partial\psi} - \Delta + (1-\beta)\nabla^2 u, \tag{2.9}$$

$$Re\left(\frac{\partial v}{\partial t} + u\rho\frac{\partial v}{\partial\rho} - v\frac{\partial v}{\partial\psi}\right) = \frac{\partial p}{\partial\psi} + \rho\frac{\partial\zeta}{\partial\rho} - \frac{\partial\Gamma}{\partial\psi} + (1-\beta)\nabla^2 v, \tag{2.10}$$

$$Re\left(\frac{\partial w}{\partial t} + u\rho\frac{\partial w}{\partial\rho} - v\frac{\partial w}{\partial\psi}\right) = \rho\frac{\partial\gamma}{\partial\rho} - \frac{\partial\Pi}{\partial\psi} + (1-\beta)\nabla^2 w, \tag{2.11}$$

$$\Sigma + We\frac{\partial \Sigma}{\partial t} = -We\left(u\rho\frac{\partial \Sigma}{\partial \rho} - v\frac{\partial \Sigma}{\partial \psi} - 2\rho\frac{\partial u}{\partial \rho}\Sigma + 2\frac{\partial u}{\partial \psi}\zeta\right) + 2\beta\rho\frac{\partial u}{\partial \rho}, \tag{2.12}$$

$$\zeta + We\frac{\partial \zeta}{\partial t} = -We\left(u\rho\frac{\partial \zeta}{\partial \rho} - v\frac{\partial \zeta}{\partial \psi} - \Sigma\rho\frac{\partial v}{\partial \rho} + \Gamma\frac{\partial u}{\partial \psi}\right) + \beta\left(\rho\frac{\partial v}{\partial \rho} - \frac{\partial u}{\partial \psi}\right), \tag{2.13}$$

$$\gamma + We\frac{\partial \gamma}{\partial t} = -We\left(u\rho\frac{\partial \gamma}{\partial \rho} - v\frac{\partial \gamma}{\partial \psi} - \Sigma\rho\frac{\partial w}{\partial \rho} - \gamma\rho\frac{\partial u}{\partial \rho}\right) - We\left(\Pi\frac{\partial u}{\partial \psi} + \zeta\frac{\partial w}{\partial \psi}\right) + \beta\rho\frac{\partial w}{\partial \rho}, \tag{2.14}$$

$$\Gamma + We\frac{\partial \Gamma}{\partial t} = -We\left(u\rho\frac{\partial \Gamma}{\partial \rho} - v\frac{\partial \Gamma}{\partial \psi} - 2\zeta\rho\frac{\partial v}{\partial \rho} + 2\Gamma\frac{\partial v}{\partial \psi}\right) - 2\beta\frac{\partial v}{\partial \psi}, \tag{2.15}$$

$$\begin{aligned}\Pi + We\frac{\partial \Pi}{\partial t} = & -We\left(u\rho\frac{\partial \Pi}{\partial \rho} - v\frac{\partial \Pi}{\partial \psi} - \gamma\rho\frac{\partial v}{\partial \rho}\right) \\ & -We\left(-\zeta\rho\frac{\partial w}{\partial \rho} + \Pi\frac{\partial v}{\partial \psi} + \Gamma\frac{\partial w}{\partial \psi}\right) - \beta\frac{\partial w}{\partial \psi},\end{aligned} \tag{2.16}$$

and

$$\Delta + We\frac{\partial \Delta}{\partial t} = -We\left(u\rho\frac{\partial \Delta}{\partial \rho} - v\frac{\partial \Delta}{\partial \psi}\right) - 2De\left(\Pi\frac{\partial w}{\partial \psi} - \gamma\rho\frac{\partial w}{\partial \rho}\right). \tag{2.17}$$

For small α the domain now becomes to leading order

$$0 \leqslant \rho \leqslant \infty, \quad 0 \leqslant \psi \leqslant 1, \quad 0 \leqslant \theta \leqslant 2\pi.$$

The no-slip boundary conditions in this case are

$$u = v = w = 0 \quad \text{on } \psi = 0, \tag{2.18}$$

and

$$u = v = 0,\ w = 1 \quad \text{on } \psi = 1. \tag{2.19}$$

In addition, we require u, v, and w to be bounded as $\rho \to 0$ and as $\rho \to \infty$. The Laplacian is defined as

$$\nabla^2 \equiv \rho^2\frac{\partial^2}{\partial \rho^2} + \rho\frac{\partial}{\partial \rho} + \frac{\partial^2}{\partial \psi^2}.$$

The dimensionless quantities appearing above are the Deborah number $De \equiv \lambda\varpi$, the Weissenberg number $We \equiv \lambda\dot{\gamma}$, the local Reynolds number $Re \equiv (\alpha\tilde{r}^2\varpi\tilde{\rho})/\eta$, and the retardation parameter $\beta \equiv \eta_p/(\eta_s + \eta_p)$.

Equations (2.8)–(2.19) admit a viscometric solution

$$u = v = 0, \quad w = \psi, \tag{2.20}$$

$$\Sigma = \zeta = \gamma = \Gamma = 0, \quad \Pi = -\beta, \quad \Delta = 2\beta De. \tag{2.21}$$

3. Linear stability analysis

To determine the stability of the base flow we define small perturbations

$$\boldsymbol{q} = \bar{\boldsymbol{q}} + \hat{\boldsymbol{q}} \tag{3.1}$$

where $\bar{\boldsymbol{q}}$ is the base flow given by (2.20)–(2.21), and $\hat{\boldsymbol{q}}$ is the perturbation. Substituting (3.1) in (2.8)–(2.19) and linearizing we obtain the following equations in which the hats have been dropped:

$$\rho\frac{\partial u}{\partial \rho}-\frac{\partial v}{\partial \psi}=0, \tag{3.2}$$

$$Re\frac{\partial u}{\partial t}=-\rho\frac{\partial p}{\partial \rho}+\rho\frac{\partial \Sigma}{\partial \rho}-\frac{\partial \zeta}{\partial \psi}-\Delta+(1-\beta)\nabla^2 u, \tag{3.3}$$

$$Re\frac{\partial v}{\partial t}=\frac{\partial p}{\partial \psi}+\rho\frac{\partial \zeta}{\partial \rho}-\frac{\partial \Gamma}{\partial \psi}+(1-\beta)\nabla^2 v, \tag{3.4}$$

$$Re\left(\frac{\partial w}{\partial t}-v\right)=\rho\frac{\partial \gamma}{\partial \rho}-\frac{\partial \Pi}{\partial \psi}+(1-\beta)\nabla^2 w, \tag{3.5}$$

$$We\frac{\partial \Sigma}{\partial t}+\Sigma=2\beta\rho\frac{\partial u}{\partial \rho} \tag{3.6}$$

$$We\frac{\partial \zeta}{\partial t}+\zeta=\beta\left(\rho\frac{\partial v}{\partial \rho}-\frac{\partial u}{\partial \psi}\right), \tag{3.7}$$

$$We\frac{\partial \gamma}{\partial t}+\gamma=-We\left(\zeta-\beta\frac{\partial u}{\partial \psi}\right)+\beta\rho\frac{\partial w}{\partial \rho}, \tag{3.8}$$

$$We\frac{\partial \Gamma}{\partial t}+\Gamma=-2\beta\frac{\partial v}{\partial \psi}, \tag{3.9}$$

$$We\frac{\partial \Pi}{\partial t}+\Pi=-We\left(\Gamma-\beta\frac{\partial v}{\partial \psi}\right)-\beta\frac{\partial w}{\partial \psi}, \tag{3.10}$$

$$We\frac{\partial \Delta}{\partial t}+\Delta=-2De\left(\Pi-\beta\frac{\partial w}{\partial \psi}\right). \tag{3.11}$$

Note that because the Reynolds number depends on the local radius $\tilde{r}$ the system of equations (3.2)–(3.11) is not separable. However, Re is bounded and of $O(\alpha)$. Specifically, $0 \leqslant Re \leqslant (\alpha a^2 \varpi \tilde{\rho})/\eta$. For small α, Re changes very little over the domain. Therefore one may approximate the local Reynolds number by its maximum value or even the averaged value

$$\bar{Re}=\frac{1}{a}\int_0^a Re\,\mathrm{d}\tilde{r}=\frac{\alpha\varpi\tilde{\rho}}{a\eta}\int_0^a \tilde{r}^2\mathrm{d}\tilde{r}=\frac{\alpha a^2\varpi\tilde{\rho}}{3\eta}.$$

In any case, we shall fix the value of Re and then solve the linearized problem by separation of variables.

Introduce the stream function χ

$$u=\frac{\partial \chi}{\partial \psi},\quad v=\rho\frac{\partial \chi}{\partial \rho},$$

and seek separated solutions of the form

$$(\chi, w)=\rho^{\mathrm{i}k}\mathrm{e}^{\sigma t}(De\,q_1, q_2),$$

$$(p,\Sigma,\zeta,\gamma,\Gamma,\Pi,\Delta)=\rho^{\mathrm{i}k}\mathrm{e}^{\sigma t}(q_3,q_4,q_5,q_6,q_7,q_8,q_9)$$

where $q_i=q_i(\psi)$, k is positive and σ may be complex. First solve equations (3.6)–(3.11) for $q_4 \cdots q_9$, substitute these in (3.3)–(3.5) and eliminate p to obtain the following equations:

$$(\mathrm{D}^2-k^2)^2 q_1+a_{11}\mathrm{D}^2 q_1+a_{12}q_1+a_{13}\mathrm{D}^2 q_2=0, \tag{3.12}$$

$$(\mathrm{D}^2 - k^2)q_2 + a_{21}q_2 + a_{22}(\mathrm{D}^2 - k^2)q_1 + a_{23}q_1 = 0, \tag{3.13}$$

and boundary conditions

$$q_1 = q_1' = 0 \quad \text{for} \quad \psi = 0, 1 \tag{3.14}$$

$$q_2 = 0 \quad \text{for} \quad \psi = 0, 1. \tag{3.15}$$

Here $\mathrm{D} \equiv \mathrm{d}/\mathrm{d}\psi$. The coefficients† above are

$$a_{11} = \frac{\omega(1+\omega)\mathscr{E}_2}{F} - \frac{2\mathrm{i}k\beta(\omega+3)\mathscr{E}_1}{(\omega+1)^2 F}, \tag{3.16}$$

$$a_{12} = -\omega(\omega+1)k^2\mathscr{E}_2/F, \tag{3.17}$$

$$a_{13} = \frac{2\beta(\omega+2)}{(\omega+1)F}, \tag{3.18}$$

$$a_{21} = \omega(1+\omega)\mathscr{E}_2/F, \tag{3.19}$$

$$a_{22} = \frac{\mathrm{i}k\beta\mathscr{E}_1}{(\omega+1)F}, \tag{3.20}$$

$$a_{23} = -\mathrm{i}k(\omega+1)\mathscr{E}_1\mathscr{E}_2/F, \tag{3.21}$$

where $\omega = \sigma We$, and $F = \omega(\beta - 1) - 1$. There are two dimensionless groups in (3.12) and (3.13), namely

$$\mathscr{E}_1 \equiv DeWe, \qquad \mathscr{E}_2 \equiv Re/We.$$

Note that we may also write $\mathscr{E}_2 = (DeE)^{-1}$ where the local Ekman number $E \equiv \eta/(\alpha^2\tilde{r}^2\varpi\tilde{\rho})$. The base flow is stable if $Re(\omega) < 0$ and unstable if $Re(\omega) > 0$. Note that if we introduce a new independent variable $z = \psi - 1/2$, equations (3.12) and (3.13) and boundary conditions (3.14), (3.15) remain unchanged except that the boundary is now at $z = \pm 1/2$. In this variable the linear boundary value problem has both even and odd solutions. Since we are interested in the first eigenvalue of the problem we shall restrict our subsequent analyses to finding only even solutions.

3.1. $\mathscr{E}_2 \ll 1$: *a perturbation approach*

In many applications $\mathscr{E}_2$ is very small. For example in the experiments of McKinley *et al.* (1991) the maximum Reynolds number recorded corresponds to $E^{-1} \leqslant 0.0023$. So for a typical value of the Deborah number at criticality (e.g. $De = 1.5$) this gives $\mathscr{E}_2 \simeq 10^{-3}$. For $\mathscr{E}_2 = 0$ equations (3.12)–(3.15) can be solved exactly. Note that since $\mathscr{E}_2 = \alpha Re/De, \mathscr{E}_2$ may be small for a Reynolds number of order unity provided the gap angle α is small enough. In Olagunju (1995*b*) it was shown that the neutral stability surface for $Re = 0$, corresponding to the smallest eigenvalue, is given by

$$\mathscr{E}_1^c = \mathscr{E}_{10}, \tag{3.22}$$

$$\mathscr{E}_{10} = \frac{\Lambda}{k}\frac{\omega_0(2-\beta)[(\beta-1)\omega_0^2+1]}{\beta[(\beta-1)\omega_0^2+3-2\beta]} \tag{3.23}$$

and Λ is the value of $a_{11} - a_{13}a_{22}$ when $\mathscr{E}_2$ is zero. On this surface $\omega = \mathrm{i}\omega_0$ is purely imaginary and ω_0 is the real root of the equation

$$(1-\beta)^3\omega_0^6 + (1-\beta)(5\beta^2 - 13\beta + 7)\omega_0^4 + (3 - 7\beta + 7\beta^2 - 2\beta^3)\omega_0^2 + 2\beta - 3 = 0 \tag{3.24}$$

† Some results for the upper convected Maxwell case ($\beta = 1$) were reported in Olagunju (1996). There are typographical errors in the coefficients a_{11}, a_{12}, and a_{21} reported there.

	$\beta = 1$		$\beta = 0.75$	
k	$\mathscr{E}_{11}$	ω_1	$\mathscr{E}_{11}$	ω_1
2.9	−0.329209	−0.011949	−0.880752	−0.024493
3.1	−0.325844	−0.012093	−0.872229	−0.024538
3.3	−0.323690	−0.012165	−0.866879	−0.024465
3.5	−0.322444	−0.012167	−0.863903	−0.024277
3.7	−0.321844	−0.012102	−0.862603	−0.023980
3.9	−0.321644	−0.011974	−0.862327	−0.023580
4.1	−0.321603	−0.011787	−0.862432	−0.023085

TABLE 1. Values of $\mathscr{E}_{11}^c$ and ω_1 for selected values of k and β

		$N = 3$		$N = 4$	
	$\mathscr{E}_2$	$\mathscr{E}_1^c$	ω_c	$\mathscr{E}_1^c$	ω_c
(*a*)	0	21.17940	1.00001i	21.17937	1.00000i
	10^{-4}	21.17913	0.99999i	21.17909	0.99999i
	10^{-2}	21.15188	0.99857i	21.15184	0.99857i
	10^{-1}	20.91377	0.98588i	20.91373	0.98588i
	1.0	19.29941	0.87549	19.29934	0.87549i
(*b*)	0	24.48259	1.28265i	24.48254	1.28265i
	10^{-4}	24.48214	1.28263i	24.48208	1.28263i
	10^{-2}	24.43751	1.28059i	24.43749	1.28059i
	10^{-1}	24.04997	1.26258i	24.04993	1.26258i
	1.0	21.46352	1.11956i	21.46346	1.11956i
(*c*)	0	21.17941	1.00000i	21.17937	1.00000i
	10^{-4}	21.17930	0.99999i	21.17925	0.99999i
	10^{-2}	21.16793	0.99928i	21.16789	0.99928i
	10^{-1}	21.06754	0.99288i	21.06750	0.99288i
	1.0	20.31642	0.93535i	20.31638	0.93535i

TABLE 2. Values of $\mathscr{E}_1^c$ and ω_c for $k = 3.1$ and (*a*) $\beta = 1.0$, (*b*) $\beta = 0.75$, (*c*) $\beta = 0.5$

which minimizes $\mathscr{E}_{10}$. To obtain the neutral surfaces for $\mathscr{E}_2 \ll 1$ we use a perturbation method. Expand as follows:

$$\mathscr{E}_1^c = \mathscr{E}_{10} + \mathscr{E}_{11}\mathscr{E}_2 + o(\mathscr{E}_2) \tag{3.25}$$

and

$$\omega_c = \mathrm{i}(\omega_0 + \omega_1\mathscr{E}_2 + o(\mathscr{E}_2)). \tag{3.26}$$

In order to obtain the correction terms we substitute (3.25) and (3.26) into (3.12) and (3.13) and equate coefficients of the same powers of $\mathscr{E}_2$. This gives a set of equations which can be solved recursively. The leading-order equations are homogeneous and possess non-trivial solutions. Higher-order equations are non-homogeneous and have solutions only if certain solvability conditions are satisfied. Applying these conditions for the $O(\mathscr{E}_2)$ equations yields the values of ω_1 and $\mathscr{E}_{11}$. Higher-order corrections may be calculated the same way if desired. The values of $\mathscr{E}_{11}$ and ω_1 for selected values of k and β are given in table 1.

The preceding results show that the critical values of both $\mathscr{E}_1$ and ω decrease with $\mathscr{E}_2$ indicating that inertia destabilizes the flow and that the speed of the most unstable wave decreases with increasing inertia.

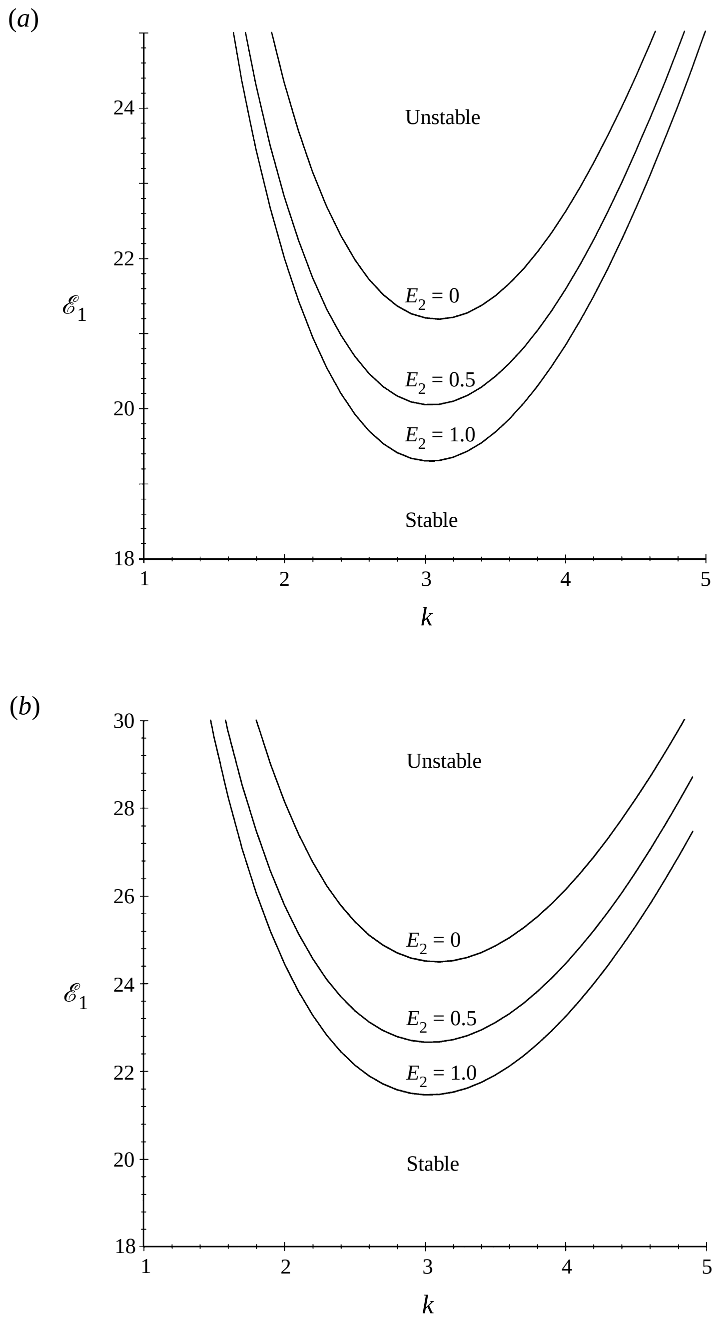

FIGURE 1 (a, b). For caption see facing page.

3.2. $\mathscr{E}_2 = O(1)$: *a Galerkin method*

For $\mathscr{E}_2 = O(1)$ we use a standard Galerkin method (Finlayson 1972; Fletcher 1984) to calculate the critical values of $\mathscr{E}_1$ at the onset of instability.

We expand q_1 and q_2 in terms of basis functions which satisfy the boundary

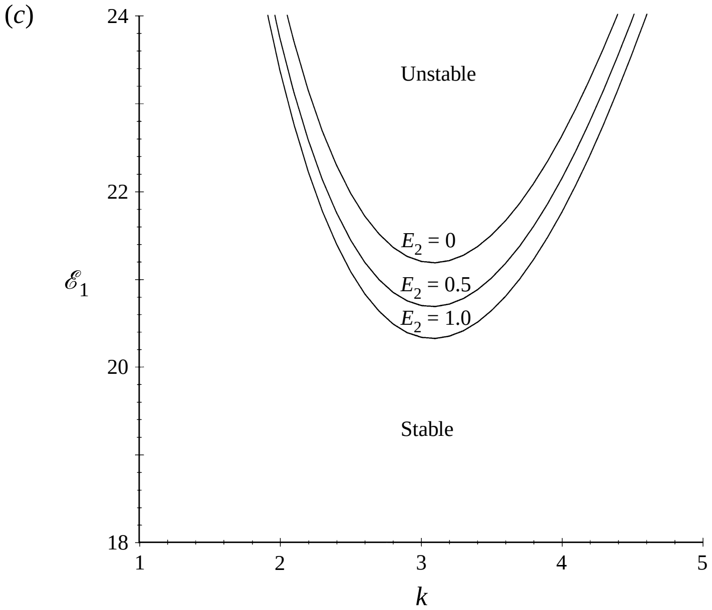

FIGURE 1. Neutral stability curves in the $(\mathscr{E}_1, k)$-plane for (*a*) $\beta = 1.0$, (*b*) $\beta = 0.75$, (*c*) $\beta = 0.5$, and selected values of $\mathscr{E}_2$.

conditions (3.14)–(3.15) as

$$q_1 = \sum_{k=1}^{N} a_k \Phi_k(z), \tag{3.27}$$

and

$$q_2 = \sum_{k=1}^{N} b_k \Psi_k(z), \tag{3.28}$$

where

$$\Phi_i(z) = (z^2 - 1/4)^2 z^{2(i-1)} \tag{3.29}$$

and

$$\Psi_i(z) = (z^2 - 1/4) z^{2(i-1)}, \tag{3.30}$$

where $z = \psi - 1/2$. Note that this choice of basis functions gives an even solution. Substituting (3.27) and (3.28) into (3.12) and (3.13) we obtain equations for the residuals

$$R_1(a_i, b_i, z) = 0 \tag{3.31}$$

and

$$R_2(a_i, b_i, z) = 0. \tag{3.32}$$

Note that we have suppressed dependence on the parameters. Proceeding in the usual way we multiply (3.31) by Φ_j and (3.32) by Ψ_j and integrate with respect to z from $-1/2$ to $1/2$ to obtain the linear system

$$\boldsymbol{M}\boldsymbol{x} = 0 \tag{3.33}$$

where $\boldsymbol{x} = (a_1, \cdots, a_N, b_1, \cdots, b_N)$ and $\boldsymbol{M}$ is a $2N \times 2N$ matrix which depends nonlinearly on the parameters. For equation (3.33) to have non-trivial solutions we must

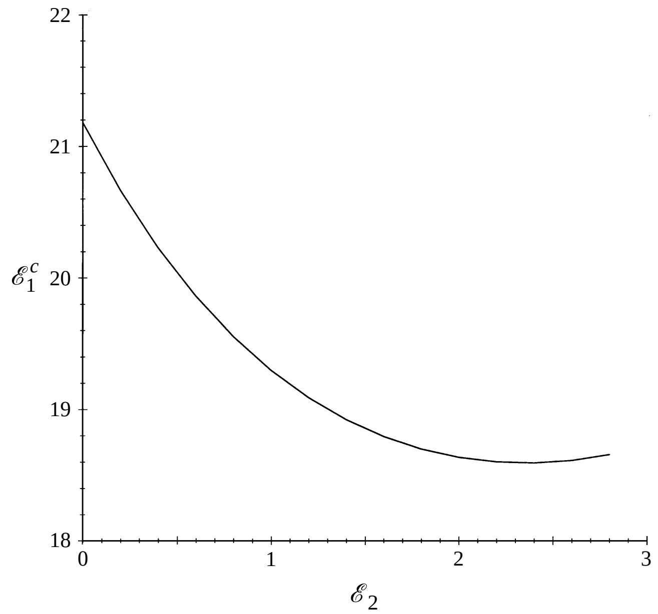

FIGURE 2. Variation of the critical elasticity number $\mathscr{E}_1^c$ with $\mathscr{E}_2$ when $\beta = 1$.

have

$$\det(\boldsymbol{M}) = 0. \tag{3.34}$$

From equation (3.34) we obtain the neutral stability curves in the $(\mathscr{E}_1, k)$-plane for any fixed value of the parameters $\mathscr{E}_2$, and β.

4. Discussion of linear stability results

The Galerkin procedure converges rapidly for a wide range of parameter values. Taking $N = 3$ in (3.27) and (3.28) we obtain values of the eigenvalue correct to three decimal places (see table 2). The neutral stability curves for selected values of the retardation parameter β and the parameter $\mathscr{E}_2$ are given in figure 1(*a–c*). As evident from the figures, for fixed values of β and $\mathscr{E}_2$, the neutral stability curve has a minimum point $(\mathscr{E}_1^c, k_c)$. For $\mathscr{E}_1$ less than $\mathscr{E}_1^c$ the base flow is linearly stable. As $\mathscr{E}_1$ increases past this value a pair of complex-conjugate eigenvalues crosses the imaginary axis into the right half-plane leading to a loss of stability. For an eigenvalue pair $(\mathrm{i}\omega_c, k_c)$ we also have the conjugate pair $(-\mathrm{i}\omega_c, -k_c)$. Note however that because the coefficients in (3.12)–(3.13) are not even functions of k the pair $(\mathrm{i}\omega_c, -k_c)$ and $(-\mathrm{i}\omega_c, k_c)$ are not eigenvalues. This means that there can be no standing wave solutions. This agrees with the results of experiments of McKinley *et al.* (1995) in which only travelling waves were observed.

From figure 2 we see that for the range of values considered $\mathscr{E}_1^c$ decreases as $\mathscr{E}_2$ increases. Thus for a fixed value of the Weissenberg number We, the flow becomes more unstable as the Reynolds number Re increases. This trend is similar to what was found for the Taylor–Dean and Taylor–Couette flows by Joo & Shaqfeh (1992, 1994). Since $\mathscr{E}_1 = De^2/\alpha$ it follows that the critical Deborah number at the onset of instability scales like $\alpha^{1/2}$.

The most unstable mode corresponds to the wavenumber k_c. This critical wavenum-

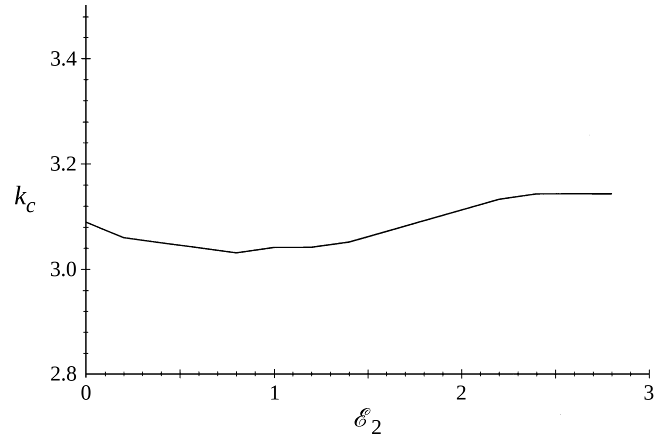

FIGURE 3. Variation of the critical wavenumber k_c with $\mathscr{E}_2$ when $\beta = 1$.

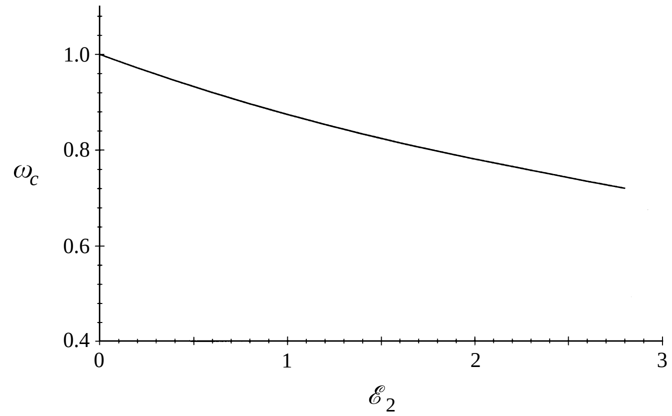

FIGURE 4. Variation of the critical frequency ω_c with $\mathscr{E}_2$ when $\beta = 1$.

ber does not change much with either β or $\mathscr{E}_2$ and is approximately $k_c = 3.1$. For the values of $\mathscr{E}_2$ considered k_c first decreases and then increases as $\mathscr{E}_2$ increases as shown in figure 3.

From the transformation $\rho^\alpha = r$, the critical eigenmode in dimensional physical variables has the form $A\mathrm{e}^{\mathrm{i}\sigma_c\dot{\gamma}\tilde{t}}\tilde{r}^{\mathrm{i}k_c/\alpha}\boldsymbol{q}(\psi)$ where A is a complex constant. Such a solution is a travelling wave propagating inwards (since $\sigma_c > 0$) towards the apex of the cone with speed (in the $\ln\tilde{r}, \tilde{t}$-plane) $c = \alpha\sigma_c\dot{\gamma}/k_c$. Since $\sigma_c = \omega_c/We$ it follows that the wave speed is $c = (\alpha\varpi\omega_c)/(k_c De_c)$ where ϖ is the angular speed of the cone. Since De_c scales like $\alpha^{1/2}$ it follows that c also scales like $\alpha^{1/2}$. The critical frequency ω_c depends on both β and $\mathscr{E}_2$. For fixed values of β, ω_c decreases as $\mathscr{E}_2$ increases showing that inertia tends to slow the waves down (see figure 4). This behaviour agrees with the results of Joo & Shaqfeh (1992, 1994) for the Taylor–Dean and Taylor–Couette flows. The dependence on the retardation parameter is more complicated. As shown in Olagunju (1995*b*), for $\mathscr{E}_2 = 0$, the critical frequency increases as β increases reaching a maximum of about 1.3 at $\beta \simeq 0.8$ and then decreases monotonically to 1 at $\beta = 1$. This general trend appears to hold for the selected values of $\mathscr{E}_2$ shown in table 3. The stream function for this critical eigenmode has infinitely many logarithmically spaced toroidal roll cells.

	$\beta = 0.25$	$\beta = 0.5$	$\beta = 0.75$	$\beta = 1$
$\mathscr{E}_2 = 0$	0.81	1.0	1.28	1.0
$\mathscr{E}_2 = 0.25$	0.80	0.98	1.23	0.97
$\mathscr{E}_2 = 0.50$	0.79	0.97	1.19	0.93
$\mathscr{E}_2 = 0.75$	0.78	0.95	1.15	0.90
$\mathscr{E}_2 = 1.0$	0.77	0.94	1.12	0.87

TABLE 3. Values of the critical frequency ω_c for selected values of $\mathscr{E}_2$ and β

5. Mechanism of instability

Purely elastic instabilities in rotational shear flows have been reported in parallel-plate flows (Byars *et al.* 1994), Taylor–Couette flow (Larson *et al.* 1990) and Taylor–Dean flow (Joo & Shaqfeh 1992). A mechanism for this type of instability was proposed by Larson *et al.* (1990) to explain the axisymmetric elastic instabilities observed in the Taylor–Couette flow of an Oldroyd-B fluid. That idea was used used by McKinley *et al.* (1995) to explain the axisymmetric elastic instability observed in cone-and-plate flow and by Joo & Shaqfeh to explain the elastic instabilities observed in Taylor–Dean flow. Joo & Shaqfeh (1992) have also used an energy analysis to explain the instability mechanism for axisymmetric and non-axisymmetric disturbances in the Taylor–Couette flow of an Oldroyd-B fluid. These analyses show that the purely elastic instabilities under consideration are driven by hoop stresses generated through the coupling between the base shearing flow, the perturbed velocity gradients and the curved streamlines.

We will show that the instability path for the problem under consideration can be explained by arguments similar to those developed by Larson *et al.* (1990) Note that in the system under consideration here (i.e. $\alpha \ll 1$), centrifugal forces are assumed to be negligible and have therefore been ignored. Consider a small perturbation in the meridional velocity gradient $\partial v/\partial \psi$. This perturbation will be reflected in the normal stress Γ which satisfies equation (3.8)

$$\Gamma + We\frac{\partial \Gamma}{\partial t} = -2\beta\frac{\partial v}{\partial \psi}. \quad (5.1)$$

This perturbation couples with the base shearing flow to produce a perturbation in the shear stress which (assuming that β is small) is given from (3.10) by

$$\Pi + We\frac{\partial \Pi}{\partial t} = -We\left(\Gamma - \beta\frac{\partial v}{\partial \psi}\right). \quad (5.2)$$

The coupling between the perturbation shear stress and the base flow further causes a perturbation in the hoop stress

$$\Delta + We\frac{\partial \Delta}{\partial t} = -2De\Pi. \quad (5.3)$$

Because the streamlines are curved this additional hoop stress enters the momentum equations which after neglecting unimportant terms are

$$Re\frac{\partial u}{\partial t} = -\rho\frac{\partial p}{\partial \rho} - \Delta + (1-\beta)\nabla^2 u \quad (5.4)$$

and

$$Re\frac{\partial v}{\partial t} = \frac{\partial p}{\partial \psi} + (1-\beta)\nabla^2 v. \tag{5.5}$$

If now we seek a separated solution of the form $u = e^{\sigma t}\rho^{ik}U(\psi)$..., using the continuity equation (3.2) and eliminating the pressure from (5.4) and (5.5), we obtain

$$(1-\beta)(D^2-k^2)^2U + \frac{2ik\beta(3+\omega)\mathscr{E}_1}{(\omega+1)^3}D^2U - \omega\mathscr{E}_2(D^2-k^2)U = 0 \tag{5.6}$$

where $D \equiv d/d\psi$ and $\omega = \sigma We$. Clearly (5.6) is a good approximation to equation (3.12) when $\beta \ll 1$. Note that in the absence of elasticity (i.e. $\mathscr{E}_1 = 0$), equation (5.6) implies that

$$\omega\mathscr{E}_2 = -\frac{(1-\beta)\int_0^1 (|D^2U|^2 + 2k^2|DU|^2)d\psi}{\int_0^1 (|DU|^2 + k^2|U|^2)d\psi} < 0. \tag{5.7}$$

It follows that elasticity is the sole destabilizing factor in the flow. Therefore the pathway to instability is the same as those for inertialess cone-and-plate flow (McKinley *et al.* 1995) and parallel plate flow (Oztekin & Brown 1993). The effect of inertia in this case is to reinforce the instability.

6. Summary

We have analysed the linear stability of axially symmetric cone-and-plate flow of an Oldroyd-B fluid when inertia is present. The stability properties are governed by two parameters: $\mathscr{E}_1 \equiv DeWe$ and $\mathscr{E}_2 \equiv Re/We$, where De, We, and Re are the Deborah, Weissenberg and Reynolds numbers respectively. For small values of $\mathscr{E}_2$ the Orr–Sommerfeld equations were solved by a perturbation method (see table 1). For selected values of $\mathscr{E}_2$ the equations were also solved using a Galerkin method. The results obtained from the two methods agree very well for $\mathscr{E}_2 \leqslant 10^{-4}$. Our results show that inertia tends to destabilize the flow. For example, for $\beta = 0.75$ and $k = 3.1$ (see table 2(*b*)) the critical value of $\mathscr{E}_1$ decreases from 24.483 for creeping flow ($\mathscr{E}_2 = 0$) to 21.463 when $\mathscr{E}_2 = 1.0$. For $\alpha = 0.1$ this gives a Deborah number of 1.56 to 1.46. The neutral curve has a parabolic shape with an absolute minimum point. For values of $\mathscr{E}_1$ less than the minimum the base flow is stable to perturbations of all wavelengths. As $\mathscr{E}_1$ increases past this critical value the flow becomes unstable as a pair of complex-conjugate eigenvalues ω crosses the imaginary axis into the right half-plane. The most unstable eigenmode gives a travelling wave solution with waves propagating inward towards the apex of the cone with infinitely many logarithmically spaced toroidal roll cells. For small values of $\mathscr{E}_2$ the critical wavenumber at the minimum point does not change much and is approximately 3.1. As $\mathscr{E}_2$ increases from zero k_c first decreases and then increases. The critical frequency ω_c on the other hand decreases monotonically with $\mathscr{E}_2$. Physically this means that as inertia increases the speed of the travelling waves decreases.

In physical variables the critical wavenumber is $\kappa = k_c/\alpha$ and thus scales like the reciprocal of the gap angle. Thus as the cone angle decreases the critical wavenumber will increase. This agrees with the observations of McKinley *et al.* (1995). The wave speed and the critical Deborah number both scale like $\alpha^{1/2}$. It follows that as the cone angle decreases the observed waves will travel more slowly. This is also in agreement with experimental observations (McKinley *et al.* 1995).

The principal mechanism responsible for this kind of instability is due to the coupling between the curved streamlines and the perturbation velocity gradients. This coupling produces additional hoop stresses which destabilize the flow.

The author would like to thank the referees for their helpful comments and suggestions. Part of this research was done while the author was on sabbatical leave at Virginia Tech. He wishes to thank Professors Robert Olin, Michael Renardy and Yuriko Renardy for their hospitality.

REFERENCES

Bird, R. B., Armstrong, R. C. & Hassager, O. 1987 *Dynamics of Polymeric Liquids*, vol. 1, 2nd Edn. John Wiley & Sons.

Byars, J. A., Oztekin, A., Brown, R. A. & McKinley G. H. 1994 Spiral instabilities in the flow of highly elastic fluids between rotating parallel disks. *J. Fluid Mech.* **271**, 171–218.

Finlayson, B. A. 1972 *The Method of Weighted Residuals and Variational Principles.* Academic.

Fletcher, C. A. J. 1984 *Computational Galerkin Methods.* Springer.

Joo, Y. L. & Shaqfeh, E. S. G. 1992 Observations of purely elastic instabilities in the Taylor–Dean flow of a Boger fluid. *J. Fluid Mech.* **262**, 22–73.

Joo, Y. L. & Shaqfeh, E. S. G. 1994 The effects of inertia on the viscoelastic Dean and Taylor–Couette flow instabilities with applications to coating flows. *Phys. Fluids* A **4**, 2415–2431.

Larson, R. G. 1992 Instabilities in viscoelastic flows. *Rheol. Acta* **31**, 213–263.

Larson, R. G., Shaqfeh, E. S. G. & Muller, S. J. 1990 A purely elastic instability in Taylor–Couette flow. *J. Fluid Mech.* **218**, 573–600.

Magda, J. J. & Larson, R. G. 1988 A transition occurring in ideal elastic liquids during shear flows. *J. Non-Newtonian Fluid Mech.* **30**, 1–19.

McKinley, G. H., Byars, J. A., Brown, R. A. & Armstrong, R. C. 1991 Observations on the inelastic instability in cone-and-plate flow of a polyisobutylene Boger fluid. *J. Non-Newtonian Fluid Mech.* **40**, 201–229.

McKinley, G. H., Oztekin, A., Byars, J. A. & Brown, R. A. 1995 Self–similar spiral instabilities in elastic flows between a cone and a plate. *J. Fluid Mech.* **285**, 23–164.

Olagunju, D. O. 1995*a* Instabilities and bifurcations of von-Kármán similarity solutions in swirling viscoelastic flow. *Z. Angew. Math. Phys.* **46**, 224–238.

Olagunju, D. O. 1995*b* Elastic instabilities in cone-and-plate flow: Small gap theory. *Z. Angew. Math. Phys.* **46**, 946–959.

Olagunju, D. O. 1996 Analytical results on stability of cone-and-plate flow for Re $\neq 0$. *XIIth Intl Congr. Rheol. Quebec, Canada.*

Olagunju, D. O. 1997 Hopf bifurcation in creeping cone-and-plate flow of a viscoelastic fluid. *Z. Angew. Math. Phys.* (to appear).

Olagunju, D. O. & Cook, L. P. 1993 Linear stability analysis of cone and plate flow of an Oldroyd-B fluid. *J. Non-Newtonian Fluid Mech.* **47**, 93–105.

Oztekin, A. & Brown, R. A. 1993 Instability of a viscoelastic fluid between rotating parallel disks: analysis for the Oldroyd-B fluid. *J. Fluid Mech.* **225**, 473–502.

Phan-Thien, N. 1985 Cone-and-plate flow of the Oldroyd-B fluid is unstable. *J. Non-Newtonian Fluid Mech.* **17**, 37–44.